This article has been accepted for inclusion in a future issue of this journal. Content is final as presented, with the exception of pagination.

Numerical Modeling for the Underfill Flow in Flip-Chip Packaging

J. W. Wan, W. J. Zhang, and D. J. Bergstrom

***Abstract*—In the prediction of underfill flow in a flip-chip package, numerical methods are usually used for flow analysis and simulation since analytical methods cannot meet the requirement for predicting fluid distribution in a planar analysis. At present, there appears to be no simulation software commercially available that is able to provide adequate prediction for the underfill flow process driven by capillary force in a micro-cavity situation. In the study presented in this paper, a numerical model was proposed for the prediction of flip-chip underfill flow. In this model, the power-law constitutive equation was used to describe the non-Newtonian behavior of encapsulant fluids and a time-dependent velocity boundary condition was used instead of the pressure boundary condition commonly used. The comparison between the model-predicted and experimental results indicated that this model can give a good prediction for the underfill flow in a micro-cavity. This model was implemented by a general-purpose commercially available software program ANSYS, which has a high reliability and wide accessibility.**

***Index Terms*—Flip-chip underfill flow, numerical simulation model, parallel plates, power-law constitutive equation, time-dependent velocity boundary condition.**

I. Introduction

THE underfill process is a very important manufacturing step in flip-chip packaging because of its great impact on the reliability of flip-chip packaging. Many studies have been carried out for predicting the flow characteristics using analytical or numerical methods [1]–[9]. The analytical methods usually treat the flow as a one-dimensional problem, and they are not able to describe the distribution of fluid in a two-dimensional field. Therefore, numerical methods were developed for a more accurate underfill flow analysis [4], [6], [8]. In the study reported by Nguyen *et al.* [4], the plastic integrated circuit encapsulation computer-aided design (PLICE-CAD) simulation code was developed for calculating the filling time and for simulating the flow front distribution in flip-chip packaging. In their study, the predicted motion of the flow front was slower than that of the observed flow front. They did not provide an explanation for this discrepancy. One of the possible reasons is that they treated a non-Newtonian encapsulant as a Newtonian fluid, which is not rational. In the study reported by Han and Wang [6], the Hele–Shaw approximation was used to describe the underfill flow characteristics for the encapsulant material FP4510. The Hershel–Bulkey viscosity constitutive equation was used to describe the non-Newtonian behavior of the underfill material. It was seen from their study that the discrepancy between the measured and calculated results was less than that reported by Nguyen [4] when the influence of the non-Newtonian behavior of underfill material on underfill flow is considered. However, the flow front predicted with their model was faster than the measured value [6]. No clear explanation was given for this discrepancy. Nguyen [4] speculated that the discrepancy might be related to the ratio of the spacing between the solder bump over the gap height. In other words, this ratio may affect the model accuracy.

Evidently, improved models are required. In the study presented in the present article, a two-dimensional numerical model was developed for the prediction of the underfill flow between two parallel plates and in a generic flip-chip package (or two parallel plates within which there is an array of solder bumps). In this model, the power-law constitutive equation was used to describe the non-Newtonian behavior of encapsulant fluids and a time-dependent velocity boundary was used instead of a pressure boundary. The finite-element method (FEM) was used to discretize the fluid flow equations, and the volume of fluid (VOF) technique was used to track the flow front. The model was implemented using the ANSYS software package (Version 7.0). Experimental results were used to verify the numerical model developed.

II. Numerical Model

A. Governing Equation

For a two-dimensional, incompressible flow, the continuity and the momentum equations are, respectively, given by [10]

$$\frac{\partial v_x}{\partial x} + \frac{\partial v_y}{\partial y} = 0 \tag{1}$$

$$\rho\left(\frac{\partial v_x}{\partial t} + v_x\frac{\partial v_x}{\partial x} + v_y\frac{\partial v_x}{\partial y}\right) = -\frac{\partial p}{\partial x} - \left(\frac{\partial \tau_{xx}}{\partial x} + \frac{\partial \tau_{yx}}{\partial y}\right) + \rho g_x \tag{2}$$

$$\rho\left(\frac{\partial v_y}{\partial t} + v_x\frac{\partial v_y}{\partial x} + v_y\frac{\partial v_y}{\partial y}\right) = -\frac{\partial p}{\partial y} - \left(\frac{\partial \tau_{xy}}{\partial x} + \frac{\partial \tau_{yy}}{\partial y}\right) + \rho g_y \tag{3}$$

Manuscript received December 23, 2004; revised February 06, 2006, February 28, 2007, December 24, 2007, and August 13, 2008. This work was supported by the Bureau of Science and Technology of Guangzhou Municipality (2006J1-CO281) and the Bureau of Education of Guangzhou Municipality (62017) through research grants. This work was recommended for publication by Associate Editor P. Sathyamurthy upon evaluation of the reviewers comments.

J. W. Wan is with the College of Civil Engineering, Guangzhou University, Guangzhou 510006, China.

W. J. Zhang and D. J. Bergstrom are with the Department of Mechanical Engineering, University of Saskatchewan, Saskatoon S7N 5A7, SK Canada.

Color versions of one or more of the figures in this paper are available online at http://ieeexplore.ieee.org.

Digital Object Identifier 10.1109/TCAPT.2009.2014355

1521-3331/$25.00 © 2009 IEEE

Authorized licensed use limited to: IEEE Xplore. Downloaded on March 22, 2009 at 10:30 from IEEE Xplore. Restrictions apply.

This article has been accepted for inclusion in a future issue of this journal. Content is final as presented, with the exception of pagination.

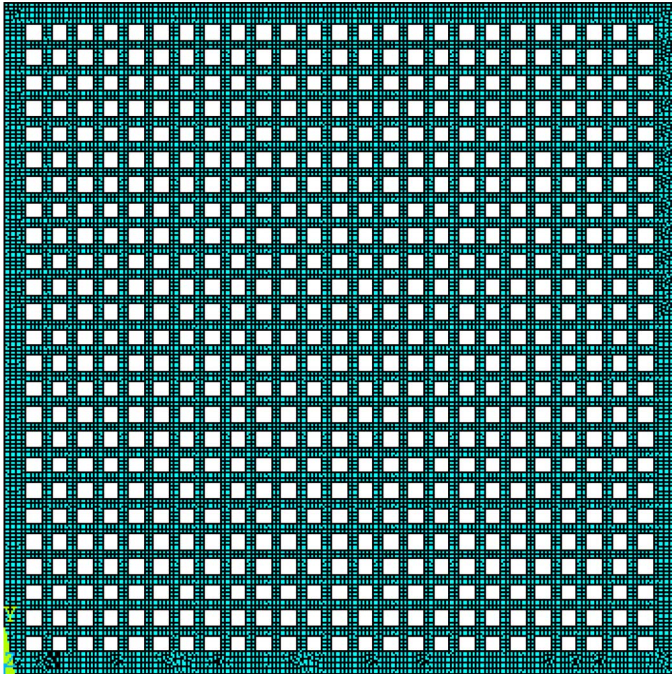

Fig. 1. Meshed geometric model of full array flip-chip underfill flow.

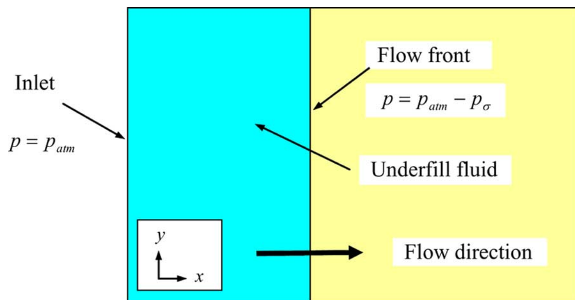

Fig. 2. Boundary conditions of the underfill flow driven by surface tension.

where v_x and v_y are the velocity components in x and y directions, respectively, p is the pressure, ρ is the fluid density, and τ is the shear stress (in which the first subscript refers to the plane on which the stress component is acting, and the second indicates the direction of the component on that plane).

The energy equation is given by

$$\rho c_v \left(\frac{\partial T}{\partial t} + v_x \frac{\partial T}{\partial x} + v_y \frac{\partial T}{\partial y}\right) = k \left(\frac{\partial^2 T}{\partial x^2} + \frac{\partial^2 T}{\partial y^2}\right) - \left(\tau_{xx}\frac{\partial v_x}{\partial x} + \tau_{yy}\frac{\partial v_y}{\partial y}\right) - \tau_{xy}\left(\frac{\partial v_x}{\partial y} + \frac{\partial v_y}{\partial x}\right) \quad (4)$$

where T is the temperature, c_v is the constant volume specific heat, and k is the thermal conductivity and taken as a constant.

B. Constitutive Equation

Most underfill materials used in flip-chip packaging show a non-Newtonian property. The study reported in [11], [12] shows that the non-Newtonian behavior of the typical underfill material used in flip-chip underfill can be described with the power-law constitutive equation, which is presented as follows [13]:

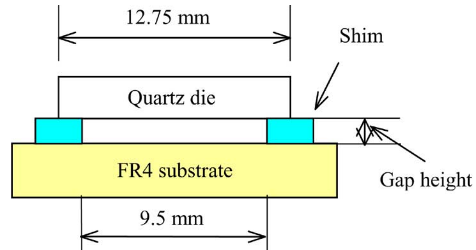

Fig. 3. Experiment setup for the underfill flow between two parallel plates.

$$\tau_{ij} = m \left|II_{2D}\right|^{(n-1)/2} (2D_{ij}) \quad (5)$$

where m and n are the coefficient and index of the power-law constitutive equation, respectively, D is the rate of deformation tensor, τ is the shear stress, and II_{2D} is the second invariant of D. The rate of deformation tensor is calculated by

$$2D = L + L^T \quad (6)$$

where L is the velocity gradient tensor, and L^T is the transpose of L, which is often written out as the dyad product of the gradient vector (symbol ∇) and the velocity vector [10]

$$\nabla \vec{V} = L^T = \sum_i \sum_j \delta_i \delta_j \frac{\partial v_j}{\partial x_i} \quad (7)$$

where δ is the unit tensor.

C. Numerical Model Development

In the study presented in this article, the VOF technique was used to track the flow front. The VOF method determines the shape and location of the free surface based on the concept of a fractional volume of fluid. In general, the evolution of the free surface is computed through the following equation

$$\frac{\partial F}{\partial t} + v_x \frac{\partial F}{\partial x} + v_y \frac{\partial F}{\partial y} = 0 \quad (8)$$

where F is defined as volume fraction (VFRC), whose value is unity at any point occupied by fluid (or liquid), and zero otherwise. This equation states that F moves with the fluid. The average value of F in a cell would then represent the fractional volume of the cell occupied by fluid. In particular, a unit value of F would correspond to a cell full of fluid, while a zero value would indicate that the cell contained no fluid. Cells with F values between zero and one indicate that the corresponding element is partially filled (called partial element) and contains a free surface. In ANSYS, an algorithm called Computational Lagrangian–Eulerian Advection Remap (CLEAR) is used to track the evolution of the free surface with time. A detailed description on the CLEAR advection algorithm can be found in the computational fluid dynamics (CFD) Guide in the ANSYS software package and in [14].

Currently, the VOF capability in ANSYS software package is available only for quadrilateral elements for two-dimensional

Authorized licensed use limited to: IEEE Xplore. Downloaded on March 22, 2009 at 10:30 from IEEE Xplore. Restrictions apply.

This article has been accepted for inclusion in a future issue of this journal. Content is final as presented, with the exception of pagination.

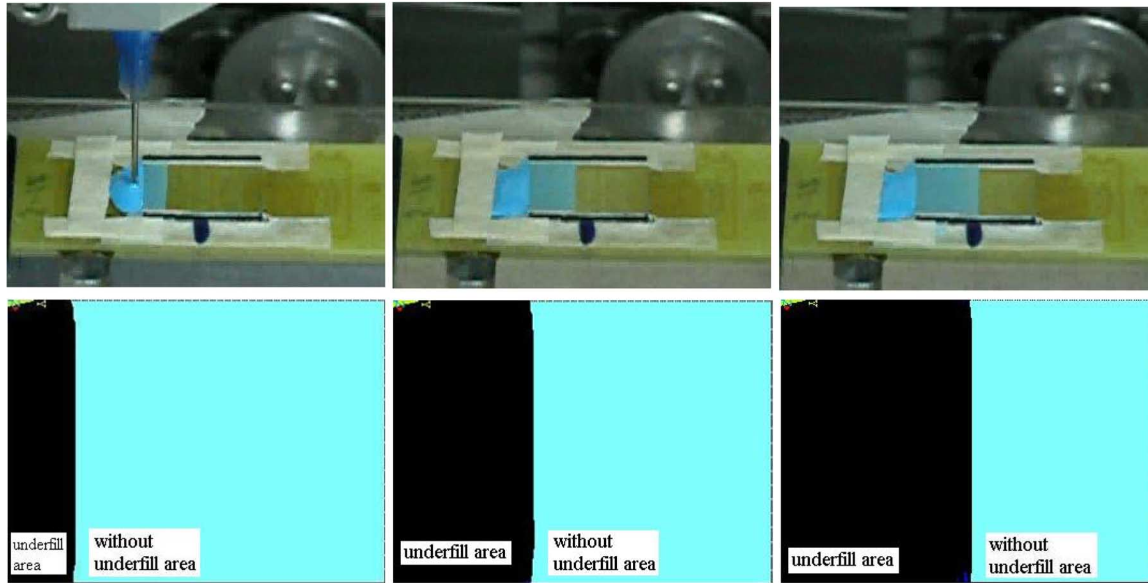

Fig. 4. Simulated flow front (bottom) compared to measured flow front (top) at filling times of 10, 30, and 50 s for a gap height of 45 μm.

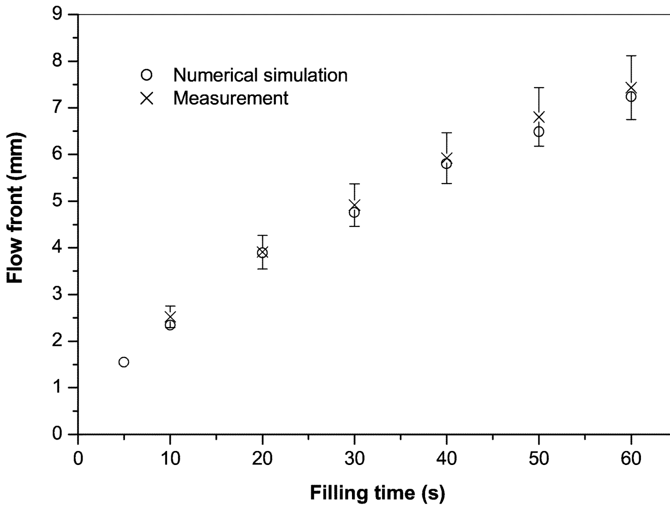

Fig. 5. Comparison of the simulated flow front with experimental results for a gap height of 45 μm.

planar or axis-symmetrical analyses. Therefore, in this study, the quadrilateral element was used in our calculation. For a flip-chip package, there are solder bumps between the substrate and the chip. The square shape was used to represent the solder bump cross section. A typical meshed geometric model for a full array of the flip-chip underfill flow is shown in Fig. 1, in which the dimension of the chip is 6.7 mm $\times$ 6.7 mm, the solder bump pitch is 250 μm, the bump width is 168 μm, and the number of solder bumps is 25 $\times$ 25. In the simulation code developed, the DO-loops structure was used to create the area of fluid flow. The quadrilateral finite-element mesh was used to perform the VOF technique to calculate the flow front position.

For an underfill flow driven by capillary action, the boundary conditions are shown in Fig. 2. At the inlet

$$p = p_{\text{atm}}. \tag{9}$$

At the flow front

$$p = p_{\text{atm}} - \Delta p_\sigma \tag{10}$$

where p_{atm} is the atmospheric pressure, and Δp_σ is the pressure change due to surface tension. On the solid walls, the velocity boundary condition is

$$\left.\begin{array}{l} v_x = 0 \\ v_y = 0 \end{array}\right\} \tag{11}$$

where v_x and v_y are the velocity components in x and y directions, respectively.

In this study, the pressure boundary condition at the inlet was converted into a time-dependent velocity function in order to consider the resistance effect of the solid surfaces of the parallel plates on the underfill flow in the two-dimensional numerical model. From the study reported in [11], the flow front position in the underfill flow is given by following equation

$$x_f = \frac{h}{2}\left(\frac{\Delta p}{m}\right)^{1/(n+1)}\left(\frac{n+1}{2n+1}t\right)^{n/(n+1)}. \tag{12}$$

By differentiating (12) with respect to time, the velocity is obtained as

$$u = \frac{nh}{2(n+1)}\left(\frac{\Delta p}{m}\right)^{1/(n+1)}\left(\frac{n+1}{2n+1}\right)^{n/(n+1)} t^{-1/(n+1)} \tag{13}$$

where u is the velocity boundary condition at the inlet, t is the filling time, h is the gap height, m and n are the coefficient and index of the power-law constitutive equation, respectively, and Δp is the driving pressure. For the underfill flow between two parallel plates Δp is calculated with the following equation [9], [15]:

$$\Delta p = \frac{2\sigma\cos\theta}{h}. \tag{14}$$

Authorized licensed use limited to: IEEE Xplore. Downloaded on March 22, 2009 at 10:30 from IEEE Xplore. Restrictions apply.

This article has been accepted for inclusion in a future issue of this journal. Content is final as presented, with the exception of pagination.

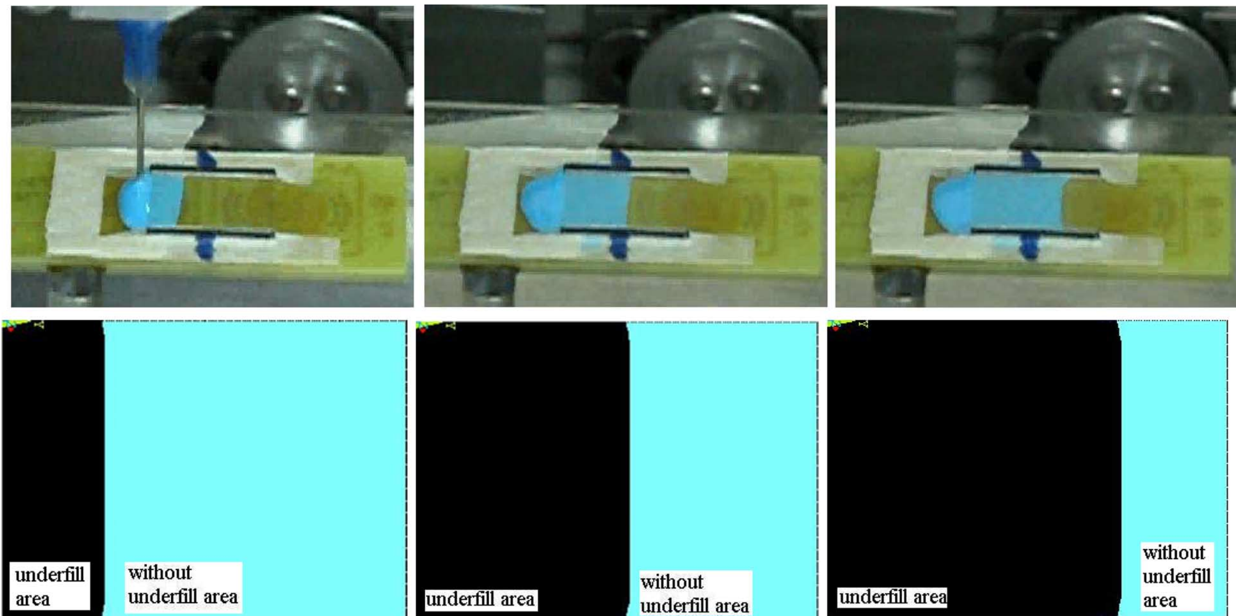

Fig. 6. Simulated flow front (bottom) compared to measured flow front (top) at filling times of 10, 30, and 50 s for the gap height of 85 μm.

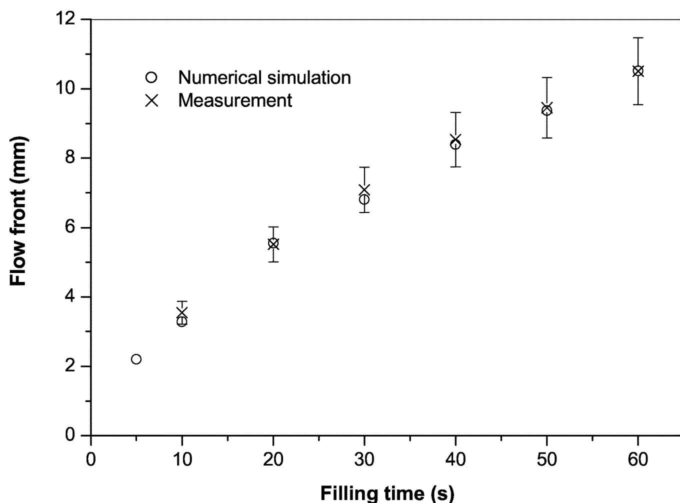

Fig. 7. Comparison of the simulated flow front with experimental results for a gap height of 85 μm.

For the flip-chip underfill flow simulation [11]

$$\Delta p = \frac{2\sigma \cos\theta (W^2 + Wd - hd)}{hW(W+d)} \tag{15}$$

where σ is the surface tension coefficient, θ is the contact angle, W is the clearance between two adjacent solder joints, h is the gap height, and d is the solder diameter. For a VOF analysis, boundary conditions are required for boundary nodes that belong to at least one non-empty (partial or full) element. It should be noted that when creating the finite-element mesh, at least two boundary nodes are required for the inlet/outlet element.

III. Model Verification

The model presented above was implemented using ANSYS software package (Version 7.0). For the discrete FEM elements, the ANSYS program calculates velocity components, pressure, and temperature from the conservation of mass, momentum, and energy.

A. *Underfill Flow Between Two Parallel Plates*

Before using the developed numerical model for simulation, experiment results were used to verify this model. The experimental setup is shown in Fig. 3. Two pieces of plastic shim stocks were placed between the quartz die and the FR4 substrate for the fluid flow between two parallel plates. Since the quartz die was transparent, the flow fronts at different times were recorded using a CCD video camera. The surface tension and contact angle in this study were measured with the DGD-ASE Contact Angle Meter, made by GBX Company, France. The viscosity was measured with a cone-and-plate rheometer (DV-III V3.3 with accuracy: $\pm 1.0\%$ of range), made by the Brookfield Engineering Laboratories, Middelboro, MA.

The numerical simulation was based on the following conditions: the plane dimension of the die was 12.75 mm $\times$ 9.5 mm, the average gap height between the chip and the substrate was 45 μm, 85 μm, and 115 μm.

The surface tension and contact angle of the simulated underfill were measured on the FR4 substrate for different temperatures between 40 °C to 90 °C. Both viscosity and surface tension are temperature-dependent and were fitted with a second-order polynomial, i.e.,

$$\sigma = 13.55113 - 0.04701T + 2.04 \times 10^{-5}T^2 \tag{16}$$

$$\theta = 88.47453 - 1.34561T + 0.00561T^2 \tag{17}$$

Authorized licensed use limited to: IEEE Xplore. Downloaded on March 22, 2009 at 10:30 from IEEE Xplore. Restrictions apply.

This article has been accepted for inclusion in a future issue of this journal. Content is final as presented, with the exception of pagination.

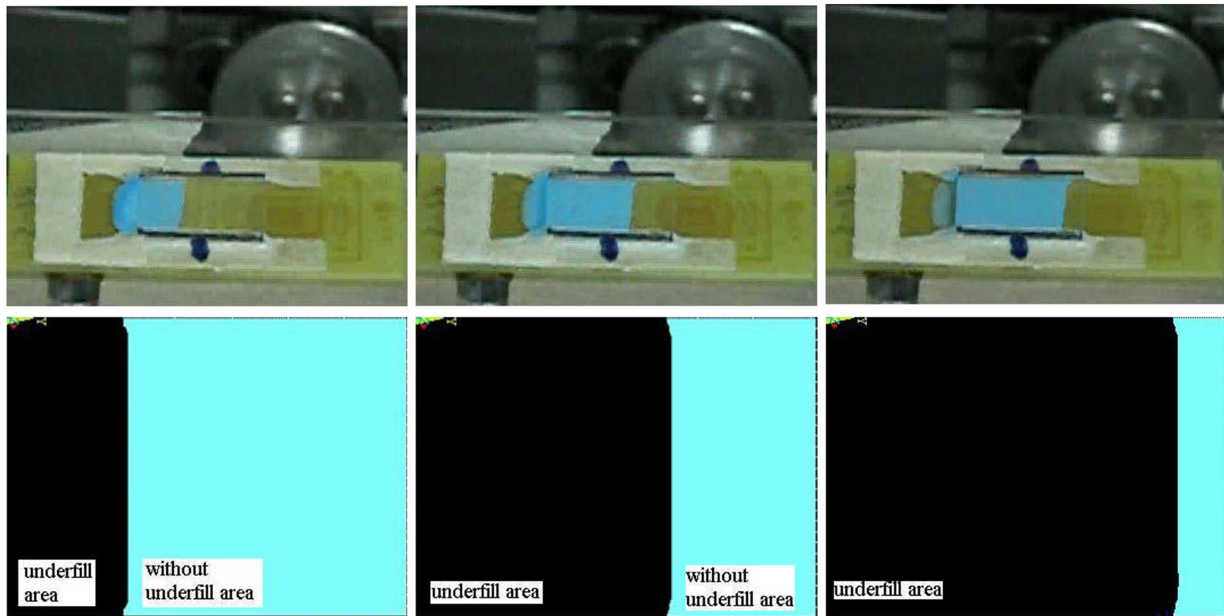

Fig. 8. Simulated flow front (bottom) compared to measured flow front (top) at filling times of 10, 30, and 50 s for the gap height of 115 μm.

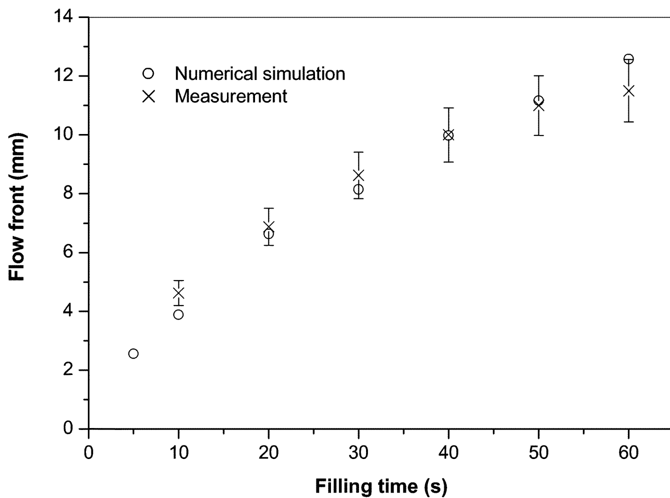

Fig. 9. Comparison of the simulated flow front with experimental results for a gap height of 115 μm.

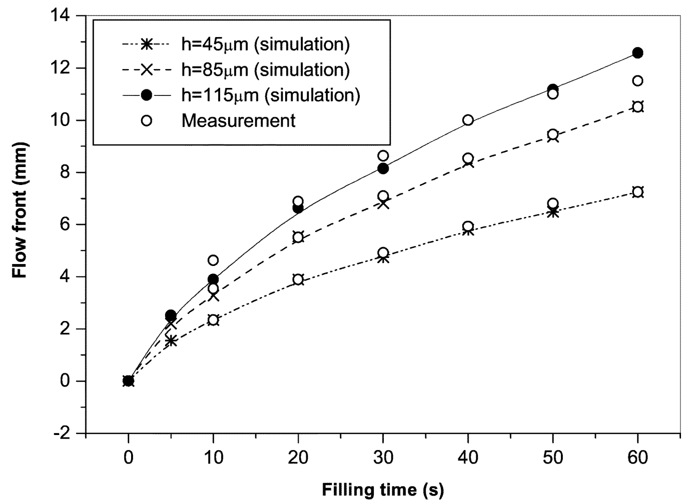

Fig. 10. Effect of gap height on filling time.

where σ is the surface tension coefficient (mN/m), θ the contact angle (degree), and T the temperature (°C). The suitable temperature range of (16) and (17) is between 30 °C and 110 °C. At 60 °C, the contact angle and the surface tension are 28.5° and 0.011 N/m, respectively.

Based on the measured data, the coefficient m and index n of the power-law constitutive equation are obtained to be 0.06 and 1.45, respectively. The density of the underfill fluid was 1800 $\mathrm{kg/m^3}$. The simulation results are shown in Fig. 4, in which the experimental results are also plotted for a comparison. Fig. 5 plots the comparison of the simulated flow front with the experimental results. From these results it can be seen that the numerical simulation results can give a good prediction for the underfill flow between two parallel plates for both the filling time and the flow front distribution. Similar results can be found in Figs. 6 and 7 for a gap height of 85 μm, and in Figs. 8 and 9 for a gap height of 115 μm.

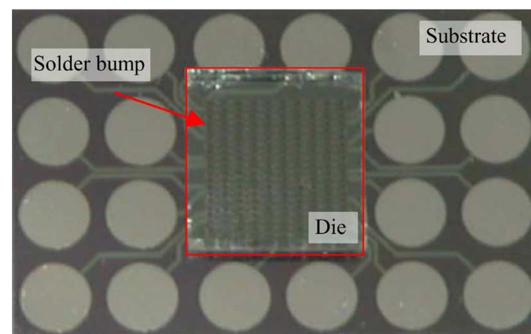

Fig. 11. Flip-chip underfill flow experiment setup.

Authorized licensed use limited to: IEEE Xplore. Downloaded on March 22, 2009 at 10:30 from IEEE Xplore. Restrictions apply.

This article has been accepted for inclusion in a future issue of this journal. Content is final as presented, with the exception of pagination.

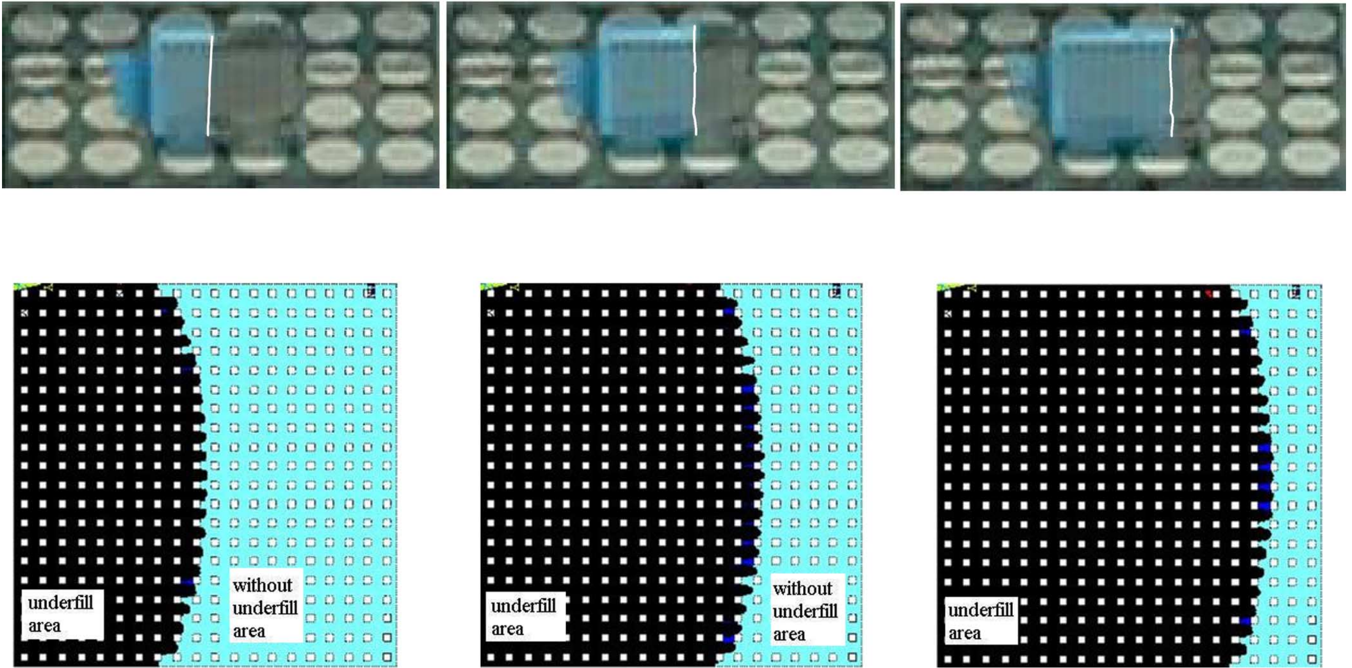

Fig. 12. Simulated flow front (bottom) compared to measured flow front (top) at filling times of 10, 20, and 30 s in flip-chip packaging.

Fig. 10 shows the influence of gap height on the filling time. From the results it can be seen that the filling time decreases with an increase in gap height.

B. Underfill Flow in Flip-Chip Package

The numerical simulation and experimental measurements were next performed for a flip-chip package. The size of the quartz die was 6 mm $\times$ 6 mm, as shown in Fig. 11. The height of the cavity gap was 50 μm, the solder bump pitch was 250 μm, and the diameter of the solder bump was 100 μm. The fitting parameters m and n of the power law model were 0.06 and 1.45, respectively, the contact angle on the FR4 substrate was 28.5°, the surface tension was 0.011 N/m, and the density was 1800 $\mathrm{kg/m^3}$.

The simulation results are shown in Figs. 12 and 13. From Fig. 12, we can see that the simulated flow front does not show a uniform profile. In order to compare the simulation results with the measurements, we chose the arithmetic mean values of maximum flow front and minimum flow front as a representative value for comparison. From the results shown in Fig. 13, it can be seen that the calculated arithmetic mean of the filling time can adequately match the measured result. However, the flow front shape does not match the measured results well. This may be because the fluid distribution in the flip-chip underfill flow is three-dimensional in nature. The simulation results show that the numerical model can still give adequate prediction for the underfill flow process in flip-chip packaging.

The model verification was also implemented with the experimental results reported in [4]. The simulation and experiment were based on the following condition: a 25 $\times$ 25 full array pattern of solder bumps connected to the quartz die and the substrate, respectively. The dimension of the die was 6.7 mm $\times$ 6.7 mm, and the average gap height between the chip and the substrate was 56 μm. The bump diameter was 168 μm and the bump pitch was 262 μm. The meshed geometric model is given in Fig. 1. In this simulation, the coefficient m and index n of the power-law constitutive equation were 1.03 and 1.09, respectively. The contact angle on the FR4 with solder mask substrate was 25.5°, and the surface tension was 0.027 N/m [4].

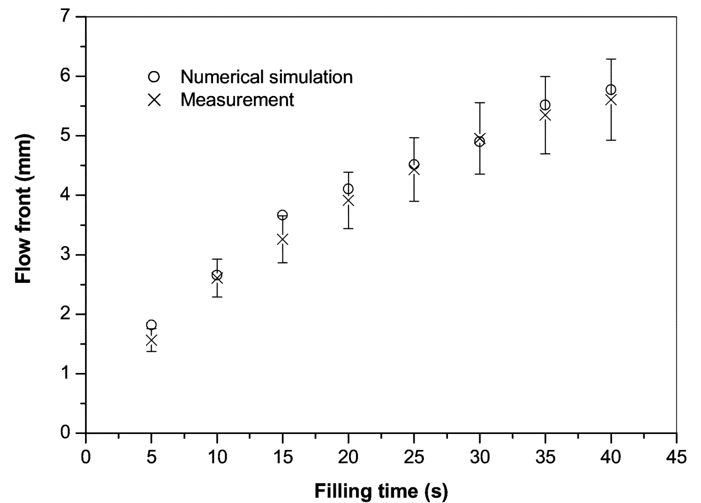

Fig. 13. Comparison of the simulated flow front with experimental results in flip-chip packaging.

Fig. 14 plots a comparison of the simulated flow front with measured flow front at different filling times of 5.3, 19.6, and 23.9 s. Due to symmetry, only half of the device is shown in Fig. 14. The right sides correspond to the measured flow front with the quartz dies reported by Nguyen *et al.* [4]. From these results, it can be seen that the predicted shapes of the flow front adequately match the measured flow fronts. Therefore, the developed model can be used to simulate the underfill flow process with good results.

Authorized licensed use limited to: IEEE Xplore. Downloaded on March 22, 2009 at 10:30 from IEEE Xplore. Restrictions apply.

This article has been accepted for inclusion in a future issue of this journal. Content is final as presented, with the exception of pagination.

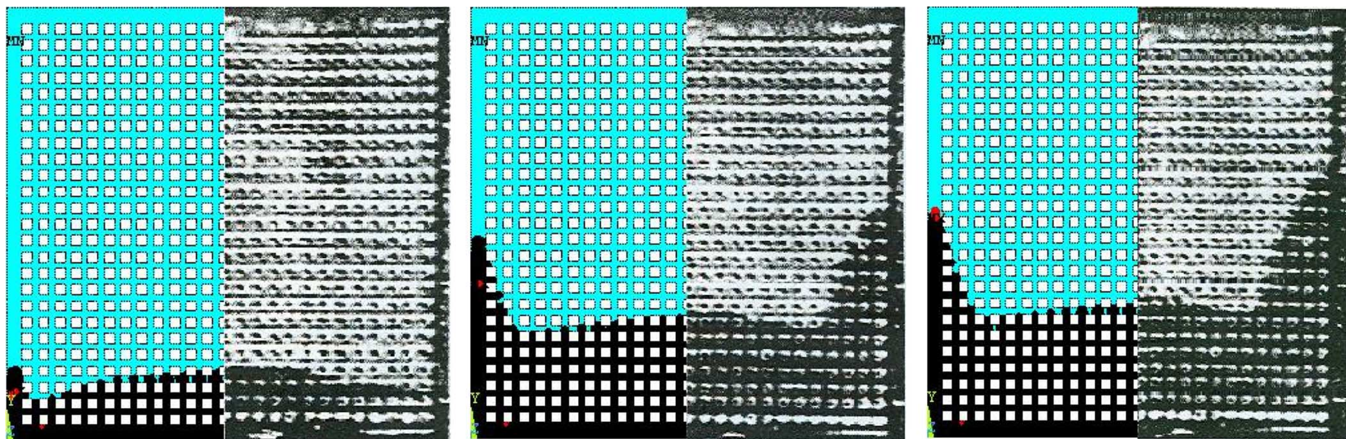

Fig. 14. Simulated flow front (left) compared to measured flow front (right) at 5.3, 19.6, and 23.9 s elapsed flow time, respectively.

A phenomenon can be observed from Fig. 14, in which there is a faster flow along the edge region, while this phenomenon is not seen from Fig. 12. This phenomenon is termed the "racing effect" by Nguyen *et al.*[4] and is caused by the wicking effect of the edge. The difference between Figs. 12 and 14 is due to the different flip-chip package settings. In Fig. 12, there is no frame surrounding the sides of the flip-chip package; the quartz die is directly placed on the solder bump. In this case, the underfill flow is not affected by the solid boundary of the frame. In Fig. 14, a frame is set around the sides of the flip-chip package [4]. The underfill flow is affected by the solid boundary of the frame and the edge width (the distance between outside solder bump and the solid boundary of the frame), which causes the racing effect.

The experimental results reported by Nguyen *et al.* [4] showed that the racing effect may form an air void in the center region of the chip. Therefore, the racing effect can significantly affect the reliability of a flip-chip package. A further numerical simulation by us shows that the racing effect is affected by the edge width. The larger the edge width, the stronger the racing effect and the less uniform the flow front. The racing effect can be reduced by decreasing the edge width.

IV. Conclusion With Further Discussion

In this study, a numerical simulation model was developed for the investigation of a two-dimensional flow front distribution. The ANSYS software package (Version 7.0) was used to implement this model. A time-dependent velocity boundary condition was employed instead of a pressure boundary condition at the inlet to consider the effect of the flow resistance caused by the solid surfaces of the parallel plates. The power-law constitutive equation was used to describe the non-Newtonian behavior of encapsulant fluids in flip-chip packaging.

The numerical model reported in this article is based on the Navier–Stokes equation for two-dimensional flow. In this numerical model, a time-dependent velocity boundary condition at the inlet was used instead of the commonly used pressure boundary condition to consider the no-slip boundary condition at the plates $z = \pm b$ (here z is gap-wise coordinate, b is one half of the gap height) to eliminate the possible error caused by other two-dimensional models employed for the three-dimensional underfill flow problem driven by capillary force. In the case of the Hele–Shaw model, in order to simplify analysis, it is assumed that the inertia term can be omitted from the momentum equation and the flow is around a single cylindrical body so that the resulting pattern of streamlines is identical with that in potential flow about the same shape [16]. Actually, in the Hele–Shaw approximation, although the no-slip boundary condition at the plates $z = \pm b$ can be satisfied, but the no-slip boundary condition at the surface of the cylindrical body is not satisfied [16]. Considering that the underfill flow in flip-chip package is affected by a set of solder bumps, the geometry is not the same as that in Hele–Shaw model and the surface resistance caused by the solder bumps may have significant influence on the flow. This effect was confirmed by the study reported by Han and Wang. In their study, the flow front calculated with a generalized Hele–Shaw model was faster than the flow front measured in their experiment for flip-chip package [6].

The numerical model described in this paper was validated using experiment, and the model can be implemented by employing commercial software, such as ANSYS. The commercial software packages used for computational fluid dynamics (CFD) are usually confirmed as reliable and relatively easy to implement. From the results reported in this study it can be seen that the developed numerical model can give a good prediction for the underfill flow between two parallel plates both for the filling time and for the flow front distribution. In the numerical simulation in flip-chip underfill flow, the calculated arithmetic average of the filling time can adequately match the measured results. However, the flow front shape does not match the measured results well, which calls for a further study.

Acknowledgment

The authors would like to thank ASM, Ltd., (Hong Kong) for providing the experimental support for this research project. The authors would also like to thank Dr. P. Liu for his helpful discussion on the research program, and Dr. D. M. Liu, Dr. J. X. Li, Dr. K. M. Lo, Dr. K. Y. Hung, Mr. K. Y. Mak, and Mr. M. Li for their excellent assistance during the experiment.

Authorized licensed use limited to: IEEE Xplore. Downloaded on March 22, 2009 at 10:30 from IEEE Xplore. Restrictions apply.

This article has been accepted for inclusion in a future issue of this journal. Content is final as presented, with the exception of pagination.

REFERENCES

[1] J. Wang, "Underfill of flip-chip on organic substrate: Viscosity, surface tension, and contact angle," *Microelectron. Rel.*, vol. 42, pp. 293–299, 2002.

[2] D. R. Gamota and C. M. Melton, "Advanced encapsulant materials systems for flip-chip on board assemblies: I. Encapsulant materials with improved manufacturing properties; II. Materials to integrate the reflow and underfilling processes," in *Proc. IEEE/CPMT Int. Electron. Manuf. Technol. Symp.*, Austin, TX, 1996, pp. 1–9.

[3] N. W. Pascarella and D. F. Baldin, "Compression flow modeling of undrefill encapsulation for low cost flip-chip assembly," *IEEE Trans. Compon., Packag., Manuf. Technol.*, vol. 21, no. 4, pt. C, pp. 325–335, Dec. 1998.

[4] L. Nguyen, C. Quentin, P. Fine, B. Cobb, S. Bayyuk, H. Yang, and S. A. Bidstrup-Allen, "Underfill of flip-chip on laminate: Simulation and validation," *IEEE Trans. Compon. Packag. Technol.*, vol. 22, no. 2, pp. 168–176, Jun. 1999.

[5] M. K. Schwiebert and W. H. Leong, "Underfill flow as viscous flow between parallel plates driven by capillary action," *IEEE Trans. Compon., Packag., Manuf. Technol. C*, vol. 19, no. 2, pp. 133–137, Apr. 1996.

[6] S. Han and K. K. Wang, "Analysis of the flow of encapsulant during underfill encapsulation of flip-chips," *IEEE Trans. Compon., Packag., Manuf. Technol.*, vol. 20, no. 4, pt. B, pp. 424–433, Dec. 1997.

[7] P. Fine, B. Cobb, and L. Nguyen, "Flip-chip underfill flow characteristics and prediction," *IEEE Trans. Compon. Packag. Technol.*, vol. 23, no. 3, pp. 420–427, Sep. 2000.

[8] M. H. Gordon, G. Ni, W. F. Schmidt, and R. P. Selvam, "A capillary-driven underfill encapsulation process," *Adv. Packag.*, vol. 8, pp. 34–37, 1999.

[9] D. S. Kim, K. C. Lee, and T. H. Know, "Micro-channel filling flow considering surface tension effect," *J. Micromech. Microeng.*, vol. 12, pp. 236–246, 2002.

[10] R. B. Bird, W. E. Stewart, and E. N. Lightfoot, *Transport Phenomena*. New York: Wiley, 1960.

[11] J. W. Wan, W. J Zhang, and D. J. Bergstrom, "An analytical model for predicting the underfill flow characteristics in flip-chip encapsulation," *IEEE Trans. Adv. Packag.*, vol. 28, no. 3, pp. 481–487, Aug. 2005.

[12] J. W. Wan, W. J. Zhang, and D. J. Bergstrom, "Experimental verification of models for underfill flow driven by capillary forces in the flip-chip package," *Microelectron. Rel.*, vol. 48, no. 3, pp. 425–430, 2008.

[13] C. W. Macosko, *Rheology: Principles, Measurements, and Applications*. New York: VCH, 1994.

[14] C. W. Hirt and B. D. Nichols, "Volume of fluid (VOF) method for the dynamics of free boundary," *J. Comput. Phys.*, vol. 39, pp. 201–225, 1981.

[15] M. J. Madou, *Fundamentals of Microfabrication- The Science of Miniaturization*. New York: CRC, 2002.

[16] H. Schlichting, *Boundary-Layer Theory*. New York: McGraw-Hill, 1979.

J. W. Wan received the M.Sc. degree in HVAC from Xi'an University of Architecture and Technology, Xi'an, China, in 1986 and the Ph.D. degree in mechanical engineering from University of Saskatchewan, Saskatoon, SK, Canada, in 2005.

He was a Visiting Scholar at the Delft University of Technology, Delft, The Netherlands, from 1990 to 1991. Currently, Dr. Wan is a Full Professor at Guangzhou University, Guangzhou, China. His current research interests include the fluid flow and heat transfer in microelectromechanical systems (MEMS) and the energy-saving technology for HVAC.

Dr. Wan is a member of the editorial board of *The Open Construction and Building Technology Journal*.

W. J. Zhang (M'01) received the Ph.D. degree in design methodology and computer aided design of mechanism systems from Delft University of Technology, Delft, The Netherlands, in 1994.

He is currently a Full Professor with the Department of Mechanical Engineering, University of Saskatchewan, Saskatoon, SK, Canada. He is also currently a Chair of Biomedical Engineering at the College of Engineering, University of Saskatchewan. He has published over 124 technical papers in refereed journals and 100 conference papers. His current research interests include electronics packaging design, applied fluids in manufacturing, biomedical technology, and biotechnology.

Dr. Zhang is a member of ASME and a senior member of ASM.

D. J. Bergstrom received the Ph.D. degree in mechanical engineering from the University of Waterloo, Waterloo, ON, Canada, in 1987.

He was appointed an Assistant Professor in the Department of Mechanical Engineering, University of Saskatchewan, Saskatoon, SK, Canada, that same year. He was promoted to Associate Professor in 1992, and Professor in 2000. As of July 1, 2004, He has been serving as Head of the Department of Mechanical Engineering. His research expertise relates to computational modeling of turbulent flows, using both Reynolds Average Navier–Stokes (RANS) models and more recently large eddy simulation techniques. Current research interests include: experimental studies of rough-wall boundary layers, two-fluid modeling of dense solid-liquid slurry flows, and fluid flow and heat transfer in microsystems.

Dr. Bergstrom is a member of the ASME and APS and is licensed as a Professional Engineer in the Province of Saskatchewan.

Authorized licensed use limited to: IEEE Xplore. Downloaded on March 22, 2009 at 10:30 from IEEE Xplore. Restrictions apply.